

# Snowfall Detection in a Foggy Scene

Hiroshi Kawarabuki

Graduate School of Science and Technology  
Hirosaki University  
Hirosaki, 036-8561, Japan  
Email:h12GS802@stu.hirosaki-u.ac.jp

Kazunori Onoguchi

Graduate School of Science and Technology  
Hirosaki University  
Hirosaki, 036-8561, Japan  
Email:onoguchi@eit.hirosaki-u.ac.jp

**Abstract**—In this paper, we propose the method for recognizing the degree of snowfall automatically even if most of backgrounds are covered with snow and the visibility is low by fog. When it snows heavily, fog often occurs simultaneously. Moreover, falling snow grains have low contrast to the background covered with white snow. In order to deal with these situations, the proposed method makes an input image clear by fog removal. We propose the novel fog removal method which can be applied to not only the usual scene but also the heavy snowy scene. This method can remove the influence of fog without depending on the grade of visibility because the degree of fog removal is changed dynamically. The degree of snowfall is estimated from the quantity of falling snow grains, which are extracted from the difference between the present defogged image and the background image created by the three-dimensional median. Experiments conducted under various degrees of snowfall have shown the effectiveness of the proposed method.

**Keywords**—Defogging; Dark channel prior; Atmospheric light; Transmission

## I. INTRODUCTION

A lot of researches which acquire the information about the weather from an image have been performed as a surveillance camera spreads. Many methods for removing the influence of the fog or the haze from an image were proposed[1]-[11]. Garg et al. [12] proposed the method of the rain detection based on characteristics that raindrops are brighter than the circumference and move linearly.

In a snowfall area, it is important to detect snow other than fog, haze or rain. Although Bossu et al. [13] proposed the method which applied rain detection to snow, this method did not have good results in a foggy scene or in a snowy background since candidates of raindrops or snow grains were extracted by the background subtraction. When it snows heavily, a background is covered with lying snow and fog often occurs. Therefore, it is necessary to detect a snowfall effectively in a foggy scene and in a snowy background.

We propose the method for recognizing the degree of snowfall automatically even if most of backgrounds are covered with snow and visibility is low because of fog or haze. At first, the proposed method makes an input image clear including snow grains by fog removal. Next, it creates the background image in which snow grains are removed from fog removal images by the three-dimensional median. Finally, the degree of snowfall is estimated from the quantity of falling snow grains, which are extracted from the difference between the present fog removal image and the background image.

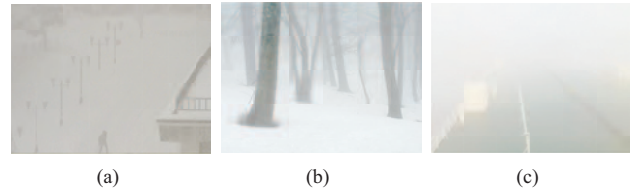


Fig. 1. Foggy scenes. (a) and (b) Snowy background; (c) The scene including a bright white object

Since conventional fog or haze removal estimates the atmospheric light which is the most haze-opaque from brightest areas, it may be chosen from a bright white area such as snow. This makes an image extremely dark or generates the wrong color. Conventional methods also make an image clear too much in a scene with good visibility. In a heavy snowfall area, the fog removal method needs to produce a natural image even in a scene covered with white areas such as snow, as shown in Fig.1 (a) and (b). It is also required not to depend on the grade of visibility since it may snow even when visibility is high. Moreover, it must be applicable to the dynamic scene in which moving objects, such as falling snow, are included.

This paper proposes the fog removal method which can remove the influence of fog from a single image in not only the usual scene but also the heavy snowy scene. The proposed method does not depend on the grade of visibility because the degree of fog removal is changed dynamically. The degree of snowfall is estimated from the fog removal image.

This paper is organized as follows. In Sect. II, related works of fog removal are reviewed briefly. In Sect. III, the outline of the proposed method is described. In Sect. IV, the dark channel prior which the proposed method uses for fog removal is explained. In Sect.V, the proposed fog removal method is described in detail. In Sect. VI, the method for estimating the degree of snowfall from fog removal images is described. In Sect. VII, experimental results obtained in various degrees of snowfall are discussed. Conclusions are presented in Sect. VIII.

## II. RELATED WORKS OF FOG REMOVAL

Fog causes degradations to the captured images. Since a degraded image loses contrast and color fidelity, this has a bad influence on outdoor image processing, for example, visual surveillance such as traffic monitoring or on-vehicle image processing. For this reason, a lot of methods for fog removal have been proposed.

Since light from the atmosphere and light reflected from an object are scattered by suspended particles such as aerosols and water droplets, the below model (1) is widely used for the formation of a foggy image:

$$I(x) = J(x)t(x) + A(1 - t(x)) \quad (1)$$

$$t(x) = e^{-\beta d(x)}, \quad (2)$$

where  $I(x)$  and  $J(x)$  are the observed intensity and the scene radiance at each pixel  $x$ ,  $A$  is the global atmospheric light,  $t(x)$  is the medium transmission describing the portion of the light reaching the camera without scattering,  $\beta$  is the scattering coefficient of the atmosphere and  $d(x)$  is the scene depth.

Restoring the scene radiance from a foggy image is ill-posed problem because the depth of the scene is unknown. In order to solve this problem, several methods used multiple images taken at the same position. Cozman et al.[1] estimated the depth from scattering by using both a fog-free image and a foggy image. Narasimhan et al. [2][3][4] obtained the scene depth and the fog removal image from two foggy images taken under different bad weather conditions. The polarization based method [5] removed the influence of fog by using multiple images taken with different degrees of polarization. These methods can not be applied to a dynamic scene including moving objects such as falling snow.

Single image fog removal is desirable to apply to the dynamic scene such as the snowfall scene. Narasimhan et al. [6] proposed the fog removal method using a single image and depth information given by a three-dimensional scene model. This method has low flexibility since it is necessary to construct a three-dimensional model beforehand.

Recently, several methods [7]-[11] using prior conditions or assumptions other than scene depth have been proposed for single image fog removal. Hautiere et al. [7][8] removed the influence of fog from a road scene by using the flat world hypothesis. This method is applicable only to the flat road scene in which the boundary of a sky and a road is included.

Tan et al. [9] created a fog-free image by maximizing contrast in a local region since a fog-free image has higher contrast than a foggy image. He et al. [10] proposed the haze removal method using dark channel prior, which assumed that at least one color channel has some pixels whose intensity are very low and close to zero in most of the nonsky region because many colorful objects and shadows are included in an outdoor scene. Tan et al. [9] used the intensity of the brightest area as the atmospheric light. He et al. [10] estimated the atmospheric light from the maximum value of the dark channel. Therefore, these methods make a white region whose intensity is higher than the atmospheric light extremely dark or give it the wrong color. Moreover, these methods need high computing cost. Tarel et al. [11] proposed the fast fog removal method which applied the edge preserving filter instead of solving an optimization problem. Since this method judges a white region whose size is larger than the filter as a foggy region, the large snow area is made clear too much.

### III. OUTLINE OF THE PROPOSED METHOD

When it snows heavily, fog often occurs simultaneously. Moreover, falling snow grains have low contrast to the background covered with white snow. In order to improve visibility of falling snow grains, our method makes an input image clear including snow grains by fog removal. Then, a background image without snow is created by applying a three-dimensional median to fog removal images. Snow grains are detected by a subtraction between the present fog removal image and the background image.

The fog removal method proposed in this paper is based on dark channel prior which He et al. [10] proposed. We realize the fog removal method equipped with the following features 1) and 2) by improving how to estimate the atmospheric light  $A$ , the relation between the dark channel and the medium transmission  $t(x)$  and how to determine the parameter  $\omega$ .

- 1) The natural defogged image, which is not made clear too much, is obtained even in the scene covered with snow.
- 2) The influence of fog is removed from a single image without depending on the grade of visibility.

### IV. DARK CHANNEL PRIOR

In this section, we briefly explain haze removal method using dark channel prior proposed by He et al [10]. This method assumes that most local regions which don't contain the sky have some pixels whose intensity is very low in at least one color channel because shadows, colorful objects or dark objects usually exist in an outdoor scene. Dehazing an image is executed based on this prior. This method uses the optical model shown in equations (1) for haze removal. Let  $R(x)$  denote a local region centered at the pixel  $x$  and  $J^c(x)$  denote a color channel of  $J(x)$ . The dark channel  $J^{dark}(x)$  is given by

$$J^{dark}(x) = \min_{y \in R(x)} \left( \min_{c \in \{R, G, B\}} J^c(y) \right). \quad (3)$$

Since this method assumes that most local regions except for the sky contains some pixels whose intensity is very low in at least one color channel,  $J^{dark}(x)$  tends to be zero.

The equation (1) changes into

$$\frac{I^c(x)}{A^c} = t(x) \frac{J^c(x)}{A^c} + 1 - t(x). \quad (4)$$

The transmission in a local region  $R(x)$  is assumed to be constant value  $\tilde{t}(x)$ . The dark channel on both sides of the equation (4) is given by

$$\min_{y \in R(x)} \left( \min_c \frac{I^c(y)}{A^c} \right) = \tilde{t}(x) \min_{y \in R(x)} \left( \min_c \frac{J^c(y)}{A^c} \right) + 1 - \tilde{t}(x). \quad (5)$$

Since  $J(x)$  is a haze-free image,  $J^{dark}(x)$  is close to zero. The equation (6) is obtained since  $A^c$  is positive.

$$\min_{y \in R(x)} \left( \min_c \frac{J^c(y)}{A^c} \right) = 0 \quad (6)$$

Therefore, the transmission  $\tilde{t}(x)$  in a local region  $R(x)$  is given by

$$\tilde{t}(x) = 1 - \omega \min_{y \in R(x)} \left( \min_c \frac{I^c(y)}{A^c} \right), \quad (7)$$

where  $\omega$  is a constant parameter between 0 and 1 which adjusts the degree of haze removal.

From equation (7), the transmission  $\tilde{t}(x)$  is estimated when the atmospheric light  $A^c$  and  $\omega$  are known. The scene radiance  $J(x)$  is obtained by assigning  $\tilde{t}(x)$  to the equation (1).

In the literature [10], the atmospheric light  $A^c$  is set up as follows and  $\omega$  is fixed to 0.95 for every scene.

- 1) The top 0.1 percent of bright pixels in the dark channel are chosen as the most haze-opaque pixels.
- 2) Among chosen pixels, pixels with highest intensity in the input image  $I$  are selected as the atmospheric light  $A$ .

## V. FOG REMOVAL METHOD

In the literature [10], the dark channel in a local region  $R(x)$  is calculated and the transmission  $\tilde{t}(x)$  is estimated, assuming that the transmission is constant in  $R(x)$ . This causes the block artifacts in the transmission map. Although they are refined by the soft matting method, this process needs high computing cost. Our method calculates the dark channel and estimates transmission  $t(x)$  in each pixel. That is, the dark channel  $I^{dark}(x)$  of each pixel  $x$  is given by

$$I^{dark}(x) = \min(I^R(x), I^G(x), I^B(x)), \quad (8)$$

where  $I^R(x)$ ,  $I^G(x)$  and  $I^B(x)$  are RGB color channels of  $I(x)$ . Since the atmospheric light  $A = (A^R, A^G, A^B)$  is the intensity of region where fog is the deepest,  $A^R(x)$ ,  $A^G(x)$  and  $A^B(x)$  are almost same intensity. Therefore, we obtain the transmission  $t(x)$  from

$$t(x) = 1 - \omega \frac{I^{dark}(x)}{A^i} \quad (9)$$

$$A^i = \frac{A^R + A^G + A^B}{3}. \quad (10)$$

Since He et al. [10] assumed that the most foggy region had the brightest dark channel, the atmospheric light was estimated from the brightest dark channel. When bright white regions exist near the camera as shown in Fig. 1 (c), the atmospheric light may become brighter than the true value since the atmospheric light may be selected from these regions. Moreover, since the transmission  $t(x)$  is a linear decreasing function with respect to the dark channel and it has the minimum value around the atmospheric light, a white object

such as snow usually have low transmission. We solve these problems by improving how to estimate the atmospheric light  $A$ , the relation between the dark channel and the medium transmission  $t(x)$  and how to determine the parameter  $\omega$ .

### A. Estimating the Atmospheric Light

The equation (1) shows that  $t(x)$  is the portion of the light reaching the camera from the object and  $1-t(x)$  is the portion of the light reaching the camera from the atmospheric light. Figure 2 (a) shows the relation of  $t(x)$  ( $1-t(x)$ ) and the dark channel  $I^{dark}(x)$ . Since  $t(x)$  is low and  $1-t(x)$  is high around the region of the atmospheric light, our method estimates the brightness of the atmospheric light in the following range:

$$I_{mid}^{dark}(x) < I^{dark}(x) < I_{max}^{dark}(x), \quad (11)$$

where  $I_{mid}^{dark}(x)$  is the dark channel at the intersection  $M$  of  $t(x)$  and  $1-t(x)$  in Fig.2 (a). When the dark channel is larger than  $I_{mid}^{dark}(x)$ , the relation of  $t(x) < 1-t(x)$  is realized. The initial value of  $A$  and  $\omega$  is set to  $I_{max}^{dark}$  and 1.  $I_{mid}^{dark}(x)$  is given by

$$I_{mid}^{dark}(x) = \frac{A}{2\omega} = \frac{I_{max}^{dark}}{2} \quad (12)$$

Since the atmospheric light covers the whole image, it is searched around the mode of the dark channel within the range of equation (11).

The search procedure of the atmospheric light is described below.

- 1) The histogram  $H^{dark}$  of the dark channel in the whole image is created.
- 2) If the mode  $I_{mode}^{dark}$  of  $H^{dark}$  satisfies  $\frac{A}{2\omega} < I_{mode}^{dark} < I_{max}^{dark}(x)$ , it goes to step 3). Otherwise, it goes to step 4).
- 3) The minimum search width  $wd$  which satisfies equations (13), (14) and (15) is determined.

$$\frac{\sum_{i=I_{mode}^{dark}-wd}^{I_{mode}^{dark}+wd} H^{dark}(i)}{\sum_{i=0}^{I_{max}^{dark}} H^{dark}(i)} > TH_{wd} \quad (13)$$

$$I_{mode}^{dark} - wd \geq \frac{A}{2\omega} \quad (14)$$

$$I_{mode}^{dark} + wd \leq I_{max}^{dark} \quad (15)$$

The threshold  $TH_{wd}$  was set as 0.25 in experiments. As shown in Fig. 2 (b), the atmospheric light is estimated in  $I_{mode}^{dark} - wd \leq W \leq I_{mode}^{dark} + wd$ . If  $wd$  satisfying the condition (13) in the range of equations (14) and (15) is not obtained, the atmospheric light is estimated in  $\frac{A}{2\omega} \leq W \leq I_{max}^{dark}$ . For all pixels whose dark channel is included in the search area  $W$ , the mean of brightness  $(I_m^R, I_m^G, I_m^B)$  is calculated every color channel. We use this mean value as the brightness of atmospheric light  $A = (A^R, A^G, A^B)$ .

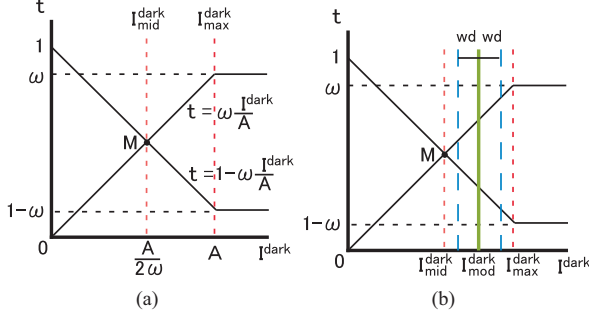


Fig. 2. Estimation of atmospheric light. (a) Relation of dark channel and transmission; (b) Search area set around the mode of dark channel

- 4) The minimum search width  $wd$  which satisfies equations (16)(17) is determined.

$$\frac{\sum_{i=I_{max}^{dark}-wd}^{I_{max}^{dark}} H^{dark}(i)}{\sum_{i=0}^{I_{max}^{dark}} H^{dark}(i)} > TH_{wd} \quad (16)$$

$$I_{max}^{dark} - wd \geq \frac{A}{2\omega} \quad (17)$$

The atmospheric light is estimated in  $I_{max}^{dark} - wd \leq W \leq I_{max}^{dark}$ . If  $wd$  satisfying the condition (16) in the range of equations (17) is not obtained, the atmospheric light is estimated in  $\frac{A}{2\omega} \leq W \leq I_{max}^{dark}$ . For all pixels whose dark channel is included in the search area  $W$ , the mean of brightness  $(I_m^R, I_m^G, I_m^B)$  is calculated every color channel. We use this mean value as the brightness of atmospheric light  $A = (A^R, A^G, A^B)$ .

### B. Relation between Transmission and Dark Channel

In a heavy snowfall area, there are a lot of objects whose dark channel is higher than the atmospheric light in the short distance. Therefore, it is necessary to set the transmission for the dark channel which is larger than the atmospheric light. A bright white region looks dark if the transmission is low. On the contrary, if the transmission is high, it looks bright because the original color of an object is incident without damping. For this reason, our method obtains the transmission  $t(x)$  at each pixel  $x$  from

$$t(x) = \begin{cases} 1 - \omega \frac{I^{dark}(x)}{A} & \text{if } 0 < I^{dark} \leq A \\ \omega \frac{I^{dark}(x)}{A} + 1 - 2\omega & \text{if } A < I^{dark} < 255 \end{cases} \quad (18)$$

As shown in Fig. 3, the equation (18) gives the same transmission if the distance from the atmospheric light  $A$  is the same. Since the transmission  $t(x)$  increases as the dark channel becomes higher than the atmospheric light, our method can suppress a phenomenon which makes a white region such as snow too clear.

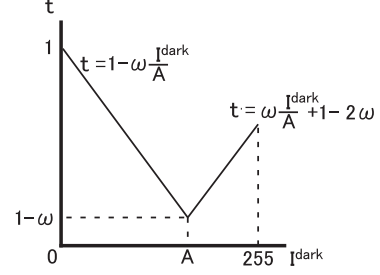


Fig. 3. Relation of dark channel and transmission

### C. Estimating the weight $\omega$

In the literature [10], the weight  $\omega$  was fixed to 0.95 for every scene. However, when defogging is applied to the fog-free image, it makes the image too dark or causes a wrong color. For the image including the near region or the image whose visibility is high, it is desirable to suppress degree of fog removal. Our method detects degree of fog automatically and controls the weight  $\omega$  dynamically. We estimate degree of fog from the histogram of the transmission in the whole image. Since a foggy image hardly includes the high transmission as shown in Fig. 4 (f), the weight  $\omega(T)$  at the present time  $T$  is determined by the bellow procedures.

- 1) The transmission  $t(x)$  is calculated by using the weight  $\omega(T-1)$  at the previous frame  $T-1$ . The weight  $\omega(0)$  at the initial frame is set as 1.
- 2) The histogram of the transmission at the present frame  $T$  is created and the number of pixels  $N_T$  whose transmission is from 0.1 to 0.4 is calculated.  $N_T$  is the total of the frequency in a red rectangle of Fig. 4.
- 3)  $\omega(T)$  is given as

$$\omega(T) = \begin{cases} 0.1 & \text{if } 0 \leq R_T < 0.2 \\ 0.7 & \text{if } 0.2 \leq R_T < 0.5 \\ 0.8 & \text{if } 0.5 \leq R_T < 0.9 \\ 0.9 & \text{if } 0.9 \leq R_T < 1.0 \end{cases} \quad (19)$$

where  $R_T$  is the ratio of  $N_T$  for the total number of pixels.

- 4) In order to avoid the rapid change of  $\omega(T)$  for the previous  $\omega(T-1)$ , the weighted average between  $\omega(T)$  and  $\omega(T-1)$  is applied:

$$\omega(T) = s\omega(T) + (1-s)\omega(T-1), \quad (20)$$

where  $s$  is the parameter which controls the degree of change. In experiments,  $s$  was set as 0.1.

The fog removal image at the present frame  $T$  is obtained by re-calculating the transmission  $t(x)$  using this  $\omega(T)$

## VI. DETECTING THE DEGREE OF SNOWFALL

The proposed method removes the influence of fog from an input image  $I_T(x)$  by the method described in the section V and judges the degree of snowfall by applying the background subtraction to the fog removal image  $I_T^d(x)$ . The background

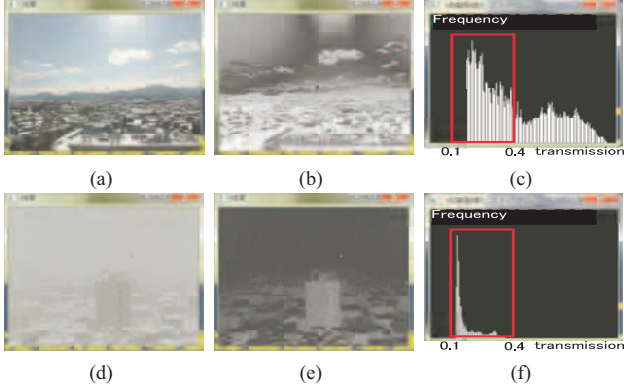


Fig. 4. Histogram of transmission. (a) Input image taken under good visibility; (b) Transmission of (a); (c) Histogram of (b); (d) Input image taken under bad visibility; (e) Transmission of (d); (f) Histogram of (e)

image  $I^B(x)$  is created by applying the three-dimensional median method to fog removal images obtained from the last  $\Delta T$  frames:

$$I^B(x) = \text{Mediam}(I_{T-\Delta T}^d(x), I_{T-\Delta T+1}^d(x), \dots, I_T^d(x)) \quad (21)$$

$I^B(x)$  is created for every color channel. The binary subtraction image  $I_T^{sb}$  between  $I_T^d(x)$  and  $I^B(x)$  is obtained from

$$I_T^{sb}(x) = \begin{cases} 1 & \text{if } \sqrt{D^{RGB}} \geq TH \\ 0 & \text{otherwise.} \end{cases} \quad (22)$$

$$D^{RGB} = (I_T^d(x)_R - I^B(x)_R)^2 + (I_T^d(x)_G - I^B(x)_G)^2 + (I_T^d(x)_B - I^B(x)_B)^2 \quad (23)$$

Logical sum is applied to the binary subtraction images  $I_{T-\Delta K}^{sb}(x), I_{T-\Delta K+1}^{sb}(x), \dots, \text{and } I_T^{sb}(x)$ . Let  $I_T^{or}(x)$  and  $R^{sb}$  denote the logical sum image and a ratio of number of pixels whose value is 1 in  $I_T^{or}(x)$  for the total number of pixels in  $I_T^{or}(x)$ . Let  $P_n$  denote the number of labels in  $I_T^{sb}(x)$  obtained by the labeling processing. The example of  $I_T^{sb}(x)$  and  $I_T^{or}(x)$  ( $K = 30$ ) is shown in Fig. 5.  $I_T^{or}(x)$  is divided into  $10 \times 10$  rectangular blocks  $B(i, j)$  ( $0 \leq i < 10, 0 \leq j < 10$ ). Let  $N^{or}(i, j)$  denote a ratio of number of pixels whose value is 1 in  $B(i, j)$  of  $I_T^{or}(x)$  for total number of pixels in  $B(i, j)$  of  $I_T^{or}(x)$  and let  $R^{or}$  denote a ratio of number of blocks which satisfy  $N^{or} > TH^{or}$  for total number of blocks. When it snows,  $P_n$ ,  $R^{sb}$  and  $R^{or}$  rise together since snow grains are detected in the whole image. On the other hand, when a moving object like a vehicle passes the scene,  $R^{or}$  do not become as high as snowfall. For this reason, our method determine the degree of snowfall by the following conditions.

if  $(P_n < thr_p \wedge R^{sb} < thr_{sb} \wedge R^{or} < thr_{or})$  no snowfall;  
 else if  $(R^{or} * R^{sb} > thr_{high})$  heavy snowfall;  
 else if  $(R^{or} * R^{sb} > thr_{medium})$  medium snowfall;  
 else if  $(R^{or} * R^{sb} > thr_{light})$  light snowfall;  
 else no snowfall;

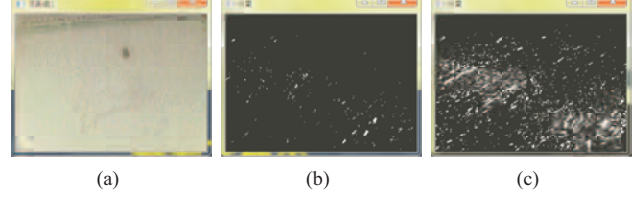


Fig. 5. Snowfall detection. (a)Input image; (b)Binary subtraction image  $I_T^{sb}(x)$ ; (c)Logical sum image  $I_T^{or}(x)$

Table I shows parameters and thresholds we used in the experiments. These were determined by experiments using images taken under various degrees of snowfall.

TABLE I. PARAMETERS AND THRESHOLDS

$thr_p$	$thr_{sb}$	$thr_{or}$	$thr_{high}$	$thr_{medium}$
2,000	0.07	0.3	0.3	0.2
$thr_{light}$	$\Delta T$	$\Delta K$	$TH$	$TH^{or}$
0.1	30	300	35	0.3

## VII. EXPERIMENTS

We conducted experiments using images taken under various degrees of snowfall. The image size was  $320 \times 240$ . Figures 6 and 7 show results of heavy snowfall, Fig.8 shows a result of medium snowfall and Fig.9 shows a result of no snowfall. In each result, the top left image is an input image, the top right image is the fog removal result obtained by He et al. [10], the bottom left image is the fog removal result obtained by the proposed method and the bottom right image is the result of snowfall detection. In Figs. 6 and 7, since most of background was covered with snow, the fog removal method using the dark channel prior [10] caused a lot of wrong colors on the snowy ground and in the sky. These areas may be detected as a snowfall wrongly. However, since the proposed method was able to suppress these errors and obtain the natural fog removal image, the degree of snowfall was judged correctly. Figures 8 and 9 are experimental results conducted under good visibility. Defogged images obtained by the dark channel prior [10] had too high chroma. However, the proposed method obtained natural results because it was able to control the degree of fog removal by adjusting the weight  $\omega$  dynamically.

We evaluated the performance of the proposed snowfall detection method using 27 scenes which consists of 1,800 frames respectively. Although these scenes were taken under various degree of snowfall (heavy snowfall:10, medium snowfall:6, light snowfall:1, no snowfall:19) and various visibility, all scenes were judged correctly. The processing time of fog removal was evaluated between the proposed method and the method proposed by He et al.[10]. Unlike He's method[10], the proposed method does not need filtering processing. Therefore, the proposed method was six times faster than He's method[10].

## VIII. CONCLUSION

In this paper, we have proposed the method for recognizing the degree of snowfall automatically even if most of backgrounds are covered with snow and the visibility of a scene is low by fog. In order to make an foggy image clear in the snowy scene, we have proposed the novel fog removal



Fig. 6. The result of heavy snowfall. Top left: Input image; Top right: Fog removal image obtained by He et al. [10]; Bottom left: Fog removal image obtained by the proposed method; Bottom right: The result of snowfall detection

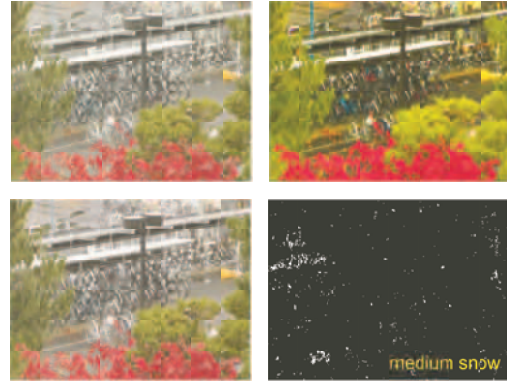


Fig. 8. The result of medium snowfall. Top left: Input image; Top right: Fog removal image obtained by He et al. [10]; Bottom left: Fog removal image obtained by the proposed method; Bottom right: The result of snowfall detection

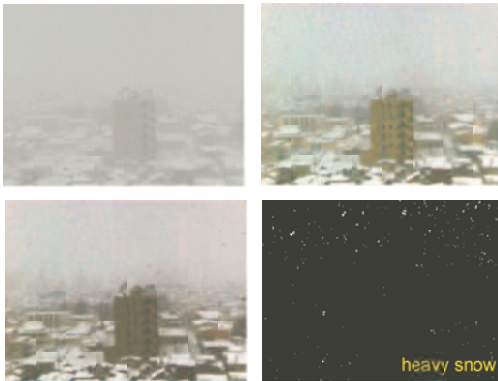


Fig. 7. The result of heavy snowfall. Top left: Input image; Top right: Fog removal image obtained by He et al. [10]; Bottom left: Fog removal image obtained by the proposed method; Bottom right: The result of snowfall detection

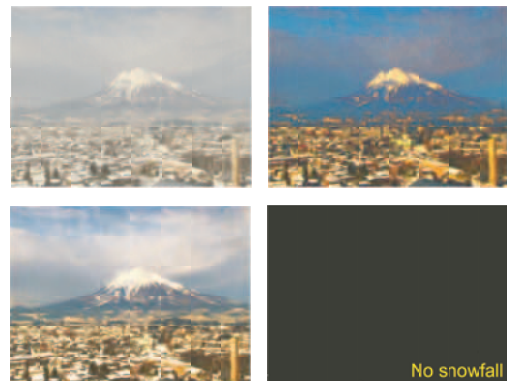


Fig. 9. The result of no snowfall. Top left: Input image; Top right: Fog removal image obtained by He et al. [10]; Bottom left: Fog removal image obtained by the proposed method; Bottom right: The result of snowfall detection

method which can be applied to not only the usual scene but also the heavy snowy scene. Experimental results obtained under various degree of snowfall have shown the usefulness of the proposed method.

Presently, the degree of snowfall is classified into four steps. We will improve it so that the quantity of more detailed snowfall may be obtained in the future.

#### REFERENCES

- [1] F. Cozman and E. Krotkov, "Depth from scattering", Proceedings of CVPR, pp.801-806, 1997.
- [2] S. G. Narasimhan and S. K. Nayar, "Vision and the Atmosphere", International Journal of Computer Vision, Vol.48, No.3, pp.233-254, 2002.
- [3] S. G. Narasimhan and S. K. Nayar, "Chromatic Framework for Vision in Bad Weather", Proceedings of CVPR, pp. 598-605, 2000.
- [4] S. G. Narasimhan and S. K. Nayar, "Contrast Restoration of Weather Degraded Images", IEEE Trans. on Pattern Analysis and Machine Intelligence, Vol.5, No.6, pp.713-724, 2003.
- [5] Y. Y. Schechner, S. G. Narasimhan and S. K. Nayar, "Instant Dehazing of Images Using Polarization", Proceedings of CVPR, pp.325-332, 2001.
- [6] S. G. Narasimhan and S. K. Nayar, "Interactive Deweathering of an Image Using Physical Models", Proceedings of IEEE Workshop on Color and Photometric Methods in Computer Vision, 2003.
- [7] H. Hautiere, J. P. Tarel and D. Aubert, "Towards fog-free in-vehicle vision systems through contrast restoration", Proceedings of CVPR, pp.1-8, 2007.
- [8] H. Hautiere, J. P. Tarel and D. Aubert, "Mitigation of visibility loss for advanced camera based driver assistances", IEEE Trans. on Intelligent Transportation Systems, vol. 11, no.2, pp. 474-484, 2010.
- [9] R. Tan, "Visibility in Bad Weather from a Single Image," Proceedings of CVPR, 2003.
- [10] K. He, J. Sun and X. Tang, "Single Image Haze Removal Using Dark-Channel Prior," IEEE Transaction on Pattern Analysis and Machine Intelligence, Vol. 33, No.12, pp.2341-2353, 2011.
- [11] J. P. Tarel and H. Hautiere, "Fast Visibility Restoration from a Single Color or Gray level Image," Proceedings of IEEE International Conference on Computer Vision (ICCV'09), pp.2201-2208, 2009.
- [12] K. Garg and S. K. Nayar, "Vision and Rain," International Journal of Computer vision, Vol.75, No.1, pp.3-27, 2007.
- [13] J. Bossu, N. Hautiere and J. P. Tarel, "Rain or Snow Detection in Image Sequences through use of a Histogram of Orientation of Streaks," International Journal of Computer vision, Vol.93, No.3, pp.348-367, 2011.